Maleic Rosin-based Gemini Surfactant as Air Entraining Agent for Concrete under Low Air Pressure

YANG LI[1,2*], ZHENDI WANG[1], LING WANG[1]

[1]State Key Laboratory of Green Building Materials, China Building Materials Academy, No.1, Guanzhuang Dongli, Chaoyang District, Beijing, China
[2]State Key Laboratory of Solid Waste Reuse for Building Materials, Beijing Building Materials Academy of Sciences Research, 69 Jinding North Street, Shijingshan District, Beijing, China

Abstract: The effectiveness of Air entraining agent (AEA) in concrete under low air pressure in the plateau area decreased. A type of new AEA, named MRE was synthesized to increase bubbles' stability in fresh concrete under low air pressure. The performance of MRE solution and concrete with MRE were tested under 60 kPa and 100 kPa compared with commercially gemini AEA (DCC). The test results showed that the foam volume of MRE and DCC solution under 60 kPa was reduced by 3% and 9% than under 100 kPa. The bubble liquid film strength of MRE is 63% higher than that of DCC. For concrete with MRE and DCC under 60 kPa, the air content was 2% and 16% lower, the relative dynamic modulus of concrete reduced by 6% and 15%, and the bubble spacing factor under 60 kPa increased by 17% and 39% respectively compared with that under 100 kPa. MRE can increase the freeze-thaw resistance of concrete under low air pressure without affecting concrete strength and is suitable for high altitude concrete.

Keywords: air-entraining agent, gemini surfactant, bubble film, low air pressure, pore structure

1. Introduction

Concrete is the most commonly used building material in the world, in which chemical admixtures [1-2] or mineral admixtures [3-5] are often added to improve its performance. Air entertaining agent (AEA) is one of chemical admixtures and is often used in concrete preparation [6]. It introduces many micrometer-sized bubbles in concrete [7] to improve fresh concrete's workability and the freeze-thaw resistance of hardened concrete [8-9]. The mainstream AEAs in applications are rosin, saponin, alkylbenzene sulfonate, and fatty alcohol sulfonate [10]. A practical problem of AEA is that its performance degenerates in a high-altitude area under low air pressure. The air content of concrete is reduced by 28 to 52%, and the bubble spacing factor of concrete increases significantly [11-12]. Further studies have shown that the performance of the AEAs with high bubble stability is less affected by the low air pressure [13]. So, an AEA with good bubble stability might be an excellent solution to this problem.

In recent years, gemini surfactants started to be used as a new type of AEA in concrete [14-15]. The gemini surfactants have higher surface activity, foamability, foam stability, and air-entraining per-formance than the corresponding single-chained surfactants [16-17]. It can be regarded as a dipolymer of two single-chain surfactants connected by a connecting group [18]. The distance between ionic groups (sulfonate, sulfate, and phosphate groups) due to electrostatic repulsion is drawn closer because of the connecting group's presence. The surfactant molecules are arranged closer at the gas-liquid interface, the surface tension of the solution decreases, and the formation bubbles' stability is improved [19-20]. These characteristics make gemini surfactants as ideal AEA for concrete under low atmospheric pressure.

Another potential solution to this problem is the rosin surfactant. Because of the ternary phenanthrene rings inside, the rosin surfactant's molecular structure is rigid, and therefore, good bubble stability would be obtained [21-22]. Simultaneously, the rosin structure contains unsaturated double bonds and carboxyl groups. So they are prone to polymerization, esterification, and other reactions [23-24].

*email:1135958226@qq.com

However, small solubility of rosin in water limits the transportation and usage of rosin AEA. Maleic anhydride is used to modify the rosin and synthesize maleic rosin [25]: Two maleic anhydrides are added to maleic rosin's molecular structure to improve its solubility. Therefore, a maleic rosin-based gemini AEA may be the right candidate for enhancing the bubbles' stability inside the concrete and reducing the effect of low air pressure on the AEA.

In this work, a new type of gemini surfactants (Tetramethylethylenediamine-dimaleic rosin gemini surfactant, hereafter abbreviated as MRE) was synthesized. The surface tension and foam volume of this surfactant were tested, the air content, strength, and freeze-thaw resistance of concrete with the gemini surfactant were tested. The results showed that MRE had excellent bubble stability and was suitable as an AEA for concrete under low atmospheric pressure.

2. Materials and methods
2.1. Materials

Maleic rosin (MS) is an industrial product. Epichlorohydrin, tetrabutylammonium bromide, anhydrous ethanol, tetramethylethylenediamine are all analytical grade chemical reagents. DCC is the commercially available gemini surfactants for comparison with MRE in this study, and its synthesis method is shown in [26]. The molecular structure of DCC is shown in Figure 1. Portland cement Type I, corresponding to EN 197, was used as the cementitious material. River sand with fineness modulus 2.8(corresponding to GBT 14684 [27]) was used as the fine aggregate. Limestone gravel was used as the coarse aggregate(meeting the requirements of national standard GBT 14685 [28]), whose mass ratio of particles with size 5-10mm to particles with size 10-20mm was 4:6. Tap water (Chloride ion content <500mg/L, sulfate content <600mg/L, meeting the requirements of standard JGJ 63 [29]) was used as the mixing water of concrete. A polycarboxylate superplasticizer with a water reduction rate of 32% and a solid content of 20% was used.
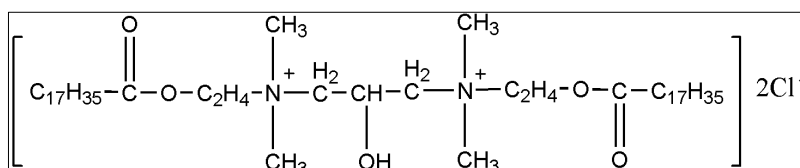

Figure 1. Chemical structure of DCC [26]

The concrete mix proportion for the test is shown in Table 1. The control concrete J had a 200mm slump at 100 kPa and air content of 4.2%, which was mainly induced by polycarboxylate super-plasticizer. The air content of the two kinds of test concrete A and B at 100 kPa was adjusted to about 7% using MRE and DCC, respectively.

Table 1. Concrete mix proportion

Concrete	Cement (kg·m^{-3})	Fine aggregate (kg·m^{-3})	Coarse aggregate (kg·m^{-3})	Water (kg·m^{-3})	Superplasticizer (kg·m^{-3})	Type and dosage of AEA (wt‰)
J						0
A	420	745	1117	168	3.14	MRE 0.10
B						DCC 0.05

2.2. Synthesis of maleic rosin gemini surfactant

The method used in the air-entraining agent MRE synthesis is an optimized method from the method in [30]. In Literature 30, rosin acid, epichlorohydrin and tetramethyl ethylenediamine were used to synthesize rosin-based gemini surfactants. However, the solubility of rosin was small, and the solubility

of synthetic surfactants was small, so it was not suitable for use as an air-entraining agent. Therefore, maleic rosin was used to instead of rosin for reaction to improve the solubility of the synthesized product. 100 g maleic rosin, 2 g tetrabutylammonium bromide, and 30 g epichlorohydrin were added to a flask. After 4 h of stirring reflux reaction at 90℃, the excess epichlorohydrin was distilled out by vacuum distillation to obtain the intermediate product of light brown liquid. The intermediate product was dissolved in anhydrous ethanol, and 6 g tetramethyl ethylenediamine was added. The magnetic stirring reflux reaction was carried out at 85℃ for 20 h. The solvent was steamed out with unreacted tetramethyl ethylenediamine, and then a dark brown liquid MRE was obtained.

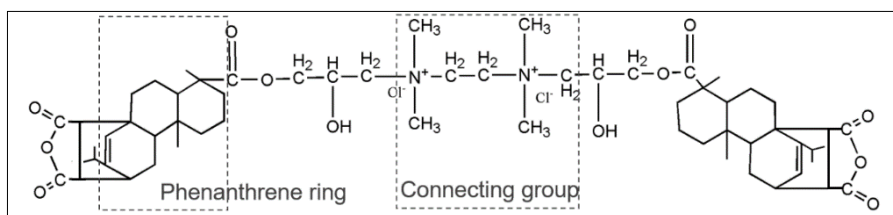The molecular structure of MRE is shown in Figure 2.

Figure 2. Chemical structure of MRE

2.3. Testing methods
2.3.1. Surface tension test

The surface tension test refered to EN 14370. The surface tension was tested using the automatic interface tension meter JZ-200A under normal pressure in Beijing. The surface tension of the AEA solution was continuously tested at the temperature was 20 ± 3℃. The surface tension of the solution was continuously measured, and the test was terminated when the standard deviation of the last five measurement data was less than 0.5 mN/m. The average of the last five measurements is the surface tension of the AEA solution.

2.3.2. Foam volume test

A solution foam performance tester [31] (Figure 3) met the requirements of ASTM D3519-88 (2007) was used to test foam volume in Beijing (100 kPa) and Lhasa (60 kPa), respectively. The stirring rake sheared the solution at high speed (rotating speed 11000 r/min) through a mixer to shear the AEA solution to produce foam. The measuring cylinder's outer diameter, inner diameter, and height is 75 mm, 65mm, and 250mm, respectively. The volume of the cylinder is about 829mL.

150mL AEA solution with a mass concentration of 0.1% was stirred for 30 s firstly, then rest for 5min before testing the remaining foam volume V. The foam volumes under 60 kPa and 100 kPa were recorded as V60 and V100, respectively.
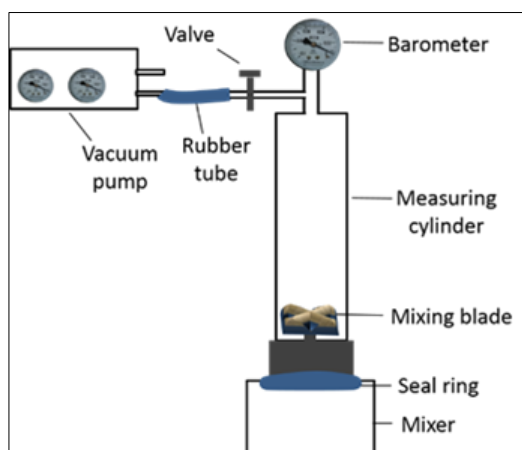

Figure 3. Foam performance tester [31]

2.3.3. Gas-liquid interface membrane structure test

The gas-liquid interface membrane structure of the air-entraining agent solution was tested with the KSV Minitrough membrane balance of Finland KSV Instrument Company. According to the literature [32], DCC and MRE were respectively formulated into 1 g·L^{-1} chloroform dilute solution. In the test, high-purity water was injected into the Langmuir tank. The surface tension was measured by the hanging piece method. A microsyringe was used to take 0.2 μL diluted chloroform solution of the air-entraining agent and spread it evenly on the water surface. After 20 min, the solvent was completely volatilized. Furthermore, a monomolecular film is formed on the air-water interface. The barrier was moved at a speed of 5 mm·min^{-1}, the surface film was compressed from both sides, and the computer records the changes in the solution area and surface pressure π. According to the number of air-entraining agent molecules added, the area occupied by each molecule can be calculated, and the π-a curve can be drawn.

The barrier is moved to the device's extreme position to obtain the extreme surface pressure of the air-entraining agent molecules. Extrapolate the steepest position in the π-a curve to obtain the limit single-molecule area. The limit surface pressure is used to characterize the strength of the air-entraining agent's monomolecular film at the gas-liquid interface. The molecular arrangement density on the bubble liquid film is inversely proportional to the limited single-molecule area. The limited single-molecule area is used to characterize the tightness of the molecular arrangement on the interface film.

2.3.4. Performance testing of concrete

The preparation of concrete was carried out in the laboratory in Beijing and Lhasa at the temperature of 20±3℃, relative humidity (RH) was 60%.

(1) Air content of concrete

The air content meter of concrete was calibrated by water to get the calibration curve in Beijing and Lhasa firstly. The well-mixed fresh concrete was poured into the air content meter bucket and vibrate. The air content of concrete was then tested and adjusted according to the calibration curve in Beijing and Lhasa.

(2) Compressive strength

Cubes of 100mm size were cast for compressive strength test. The well-mixed concretes were compacted by vibration. Then the concretes were covered with plastic sheets and kept for 24 h in laboratories (20±3℃, RH=60%). After 24 h, the concretes were demolded and transferred to a standard curing room. The concrete compressive strengths were tested at the age of 28 days in Beijing and Lhasa.

(3) Rapid freeze-thaw test of concrete

Rapid freeze-thaw test of concrete was carried out according to GBT 50082 [33]. Prismatic concrete specimens of 100mm ×100mm ×400mm were prepared for the rapid freeze-thaw test. The specimens were immersed in water at 20±2℃ for 4 days after curing for 24 days. The center temperature of the specimen was controlled at -18±2℃ to 5±2℃ during freezing and thawing. Each freeze-thaw cycle shall be completed within 2 h ~ 4 h. The relative dynamic modulus of concrete was tested after 200 freeze-thaw cycles.

(4) Pore structure of concrete

The MIC-840-01 hardened concrete pore structure analyzer produced by Japan's MARUI Company was used to test the concrete pore structure. The size of the specimen was 100mm×100 mm×100mm. After 28 days of curing (20±2℃, RH=95%), the specimen was cut at the position 20mm from the end, which creates a new surface of 100 mm×100mm. The new surface was blackened with black ink and dried in a drying cabinet. The blackened surface was then filled with white calcium carbonate powder with a particle size of less than 6.5μm. The image of the surface was collected by a camera and be analyzed by the linear method (chord length 60 mm) to obtain the pore parameters such as the number

of pores, the bubble spacing factor, the average pore diameter and pore size distribution of hardened concrete.

2.3.5. Synthetic product structure characterization

The structure of the synthesized product was characterized by the German Bruker tensor 27 infrared spectrometer. The raw materials and final products were dried at 120℃ and ground into powder for infrared testing.

3. Results and discussions
3.1. Performance of MRE
3.1.1. Surface tension

The curve of surface tension with the concentration of MRE and DCC is shown in Figure 4.
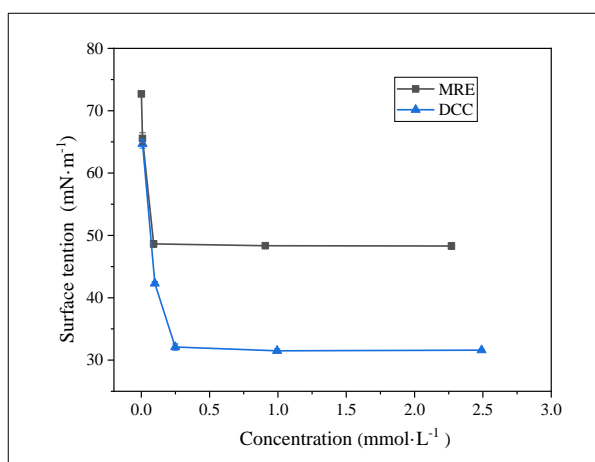

Figure 4. The relationship between surface tension and concentration of the AEAs

From Figure 4, it can be seen that the surface tension of the two solutions decreased rapidly with the increase of the concentration of the solution at the early stage. The surface tension of the solution turned out to be stable when the critical micelle concentration (CMC) was reached. The CMC of MRE and DCC were 0.09mmol/L and 0.25mmol/L, respectively. Meanwhile, the minimum surface tension corresponding to this concentration was 48.6 mN/m and 31.5 mN/m. It shows that amount of surfactant required to achieve the minimum surface tension of MRE was less than DCC, while the minimum surface tension of MRE solution was higher than DCC.

3.1.2. Foam volume

The foam volume of the tested solution under 100 kPa and 60 kPa is shown in Table 2. The foam volumes under 60 kPa and 100 kPa were recorded as V60 and V100, respectively.

Table 2. Foam volume of the surfactant under 100 kPa and 60 kPa

AEA	Foam volume (mL)		V60/V100
	V100	V60	
MRE	99	96	0.97
DCC	69	63	0.91

From Table 2, when compared with 100 kPa, the foam volume of the surfactants MRE and DCC under 60 kPa decreased by 3 and 9%, respectively. The foam stability of MRE was higher than DCC under low air pressure.

3.1.3. Gas-liquid interface membrane structure

The surface tension and bubble stability of the air-entraining agent are related to bubble liquid film structure. The π-a isotherm curves of MRE and DCC are shown in Figure 5.
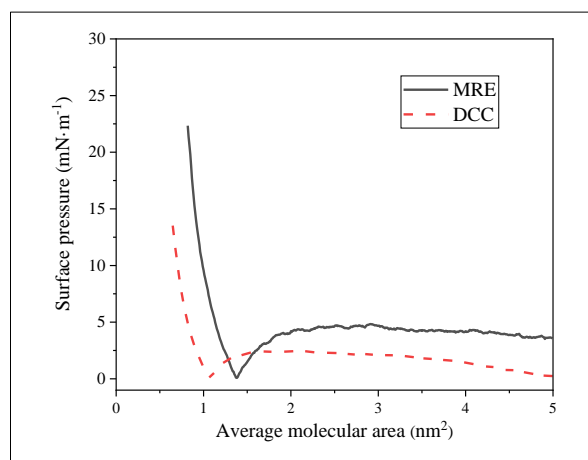

Figure 5. The π-a isotherm curves of MRE and DCC

It can be seen from Figure 5 that under the compression of the barrier, the surface pressure of MRE and DCC gradually increases. When the barrier is compressed to the limit, the surface pressures of MRE and DCC are 22.3 mN·m^{-1} and 13.7 mN·m^{-1}, respectively, indicating that the MRE bubble liquid film's strength is significantly higher than that of DCC. The limit's single-molecule area can be obtained through extrapolating from the curve slope. The limiting single-molecule areas of MRE and DCC are 0.97 nm^2 and 0.86 nm^2, respectively, indicating that DCC molecules are arranged more closely at the interface. The bubble liquid film strength of MRE is 63% higher than that of DCC, and the molecular arrangement density of MRE is 11% lower than that of DCC.

3.2. Performance of concrete with MRE
3.2.1. Air content

The air content of concrete J, A, and B tested under 60 kPa (in Lhasa) and 100 kPa (in Beijing) is shown in Table 3.

Table 3. Air content of concrete under 60 kPa and 100 kPa

Concrete	Air content (%)		The reduction rate of air content under low air pressure compared to normal pressure (%)
	100 kPa	60 kPa	
J	4.2	3.6	14
A	7.1	6.8	2
B	7.1	6.0	16

As can be seen from Table 3, compared with 100 kPa, the air content of the three concretes J, A, and B decreased by 14%, 2%, and 16%, respectively. The air content of concrete under 60 kPa is generally lower than that of 100 kPa. Compared with concrete B with DCC, low air pressure affects less on concrete A with MRE air-entraining agent.

3.2.2. Compressive strength

The 28d compressive strength of concrete tested under 60 kPa and 100 kPa is shown in Figure 6.
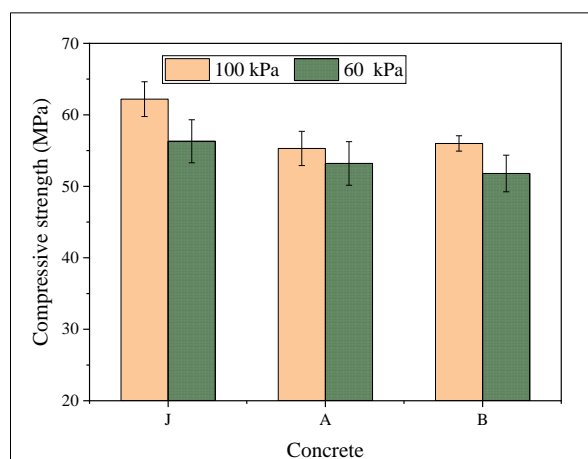
Figure 6. Compressive strength of concrete
under 60 kPa and 100 kPa

Compared with 100 kPa, the strength of concrete J under 60 kPa decreased from 62.2 MPa to 56.3 MPa; the strength of concrete A decreased from 55.3 MPa to 53.2 MPa, and the strength of concrete B decreased from 56.0 MPa to 51.8 MPa. The air content of the three concretes J, A, and B decreased by 9.5, 3.8%, and 14.8%, respectively. The compressive strength of the concrete under low air pressure was reduced compared with normal pressure.

3.2.3. Freeze-thaw resistance
The rapid freeze-thaw test results of concrete prepared and cured under 60 kPa and 100 kPa respectively are shown in Table 4.

Table 4. Relative dynamic modulus of concrete for
200 freeze-thaw cycles

Air pressure	Relative dynamic elastic modulus of concrete (%)		
	J	A	B
100 kPa	59.6	88.2	87.1
60 kPa	48.3	82.3	72.3

From Table 4, the relative dynamic elastic modulus of concrete J, A, and B under 60 kPa after 200 freeze-thaw cycles were 19%, 6%, and 15% lower than that of concrete at 100 kPa, respectively. That means the effect of increasing the freeze-thaw resistance of the AEA was reduced under 60 kPa and the decrease of freeze-thaw resistance of concrete with MRE was significantly smaller than that of other concrete.

3.3. Discussions
3.3.1. Molecular structure and characterization of MRE
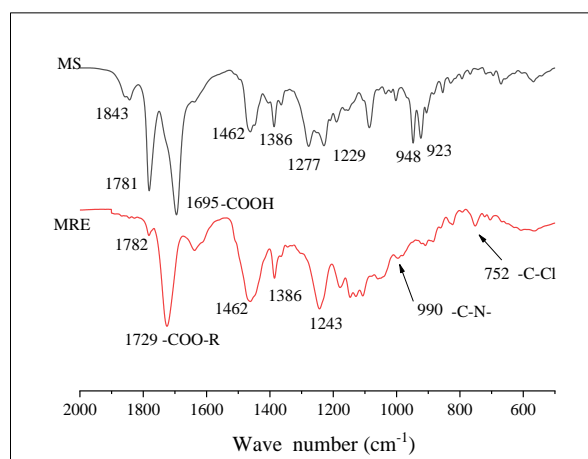The infrared spectra of maleic rosin (MS) and MRE are shown in Figure 7.

Figure 7. Infrared spectra of MS and MRE

In the MRE infrared spectrum, the 1695cm^{-1} peak disappeared, and the 1729cm^{-1} peak appeared, indicating that the carboxyl group in MS was converted to the ester group in MRE. Meanwhile, a new C-Cl stretching vibration peak appeared at 752cm^{-1}, and an absorption peak of the C-N bond appeared at 990cm^{-1} in the infrared spectrum of the MRE, which indicated the formation of the MRE of the gemini structure.

MRE contains a rosin phenanthrene ring, which makes the molecular more rigid. Compared with the DCC, the molecular structure of MRE is not easy to deform. As the data tested in 3.1.3, the larger rigid molecular arrangement density at the gas-liquid interface is relatively small, which leads to its unfavorable effect on reducing the surface tension [16]. Hence, MRE is not effective in reducing the surface tension of the solution. However, the rigid groups of MRE can form a high elastic interfacial adsorption film, which improves bubbles stability of the solution [17] and makes MRE less affected by low air pressure. Similarly, we found that the foam volume of MRE solution and the air content of concrete mixed with MRE is reduced less than normal pressure under low air pressure.

3.3.2. Pore structure of concrete with MRE

The pore structure of concrete prepared in Lhasa (60 kPa) and Beijing (100 kPa) were tested to find the reasons for the change in the strength and freeze-thaw resistance of concrete under low air pressure. Figure 8 shows the pore structure under 100 kPa and 60 kPa, and the results of the average diameter of the pores and the bubble spacing factor are shown in Table 5.
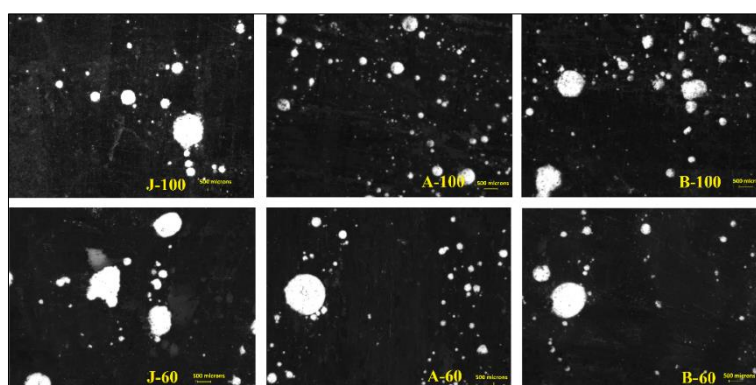

Figure 8. Image of the concrete surface
under 60 kPa and 100 kPa

Table 5. Parameters of the pore structure of hardened
concrete under 60 kPa and 100 kPa

Concrete	Average pore diameter (µm)		Bubble spacing factor(µm)	
	100kPa	60kPa	100kPa	60kPa
J	376.8	436.0	326.9	467.3
A	232.3	263.1	203.9	249.2
B	294.0	383.7	241.0	335.6

The number of pores and the pore size distribution is shown in Figure 9.
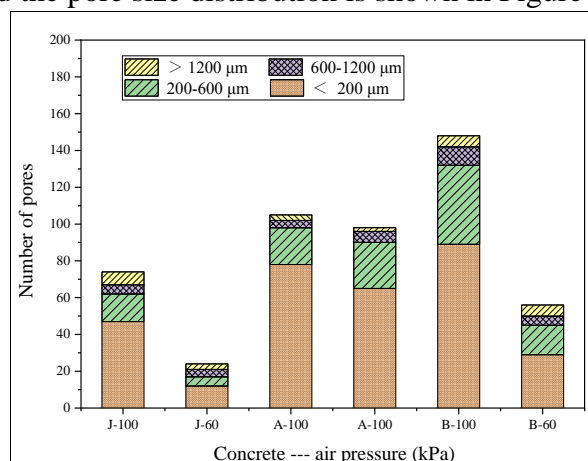

Figure 9. Pore size distribution of concrete under
60 kPa and 100 kPa

Compared with 100 kPa, the pore numbers of concrete J, A, and B decreased by 50 (from 74 to 24), 5 (from 104 to 99), and 92 (from 148 to 56) under 60 kPa respectively. The number of pores in concrete J, A, and B under 60 kPa was 68%, 5%, and 62% lower than that under 100 kPa. The number of pores in hardened concrete under 60 kPa was reduced.

The compressive strength of concrete at 28 days has strongly linked with the proportion of big pores (pore size range >1200 µm). The larger the proportion of big pores, the greater the compressive strength loss of concrete [34]. Figure 9 shows the number of big pores in concrete J, A, and B under 100 kPa and 60 kPa are 7, 3, 6, 6, 2, and 3, respectively. After calculation, the proportion of big pores in concrete J and concrete B under 60 kPa increased by 3% and 7%, respectively. Table 4, the average diameter of pores in concrete J and B under 60 kPa was 16 and 31% higher than 100 kPa, respectively. So the strength of concrete J and concrete B under 60 kPa got worse when compared with that under 100 kPa, while the average diameter of pores in concrete A under 60 kPa increased by 13% compared with that under 100 kPa. The proportion of big pores in the concrete A under 60 kPa increases by 1%. Therefore, the strength of concrete A under 60 kPa decreases slightly.

At the same time, it can be seen that the bubble spacing factor of concrete increased significantly under 60 kPa. The bubble spacing factor of concrete J, A, and B under 60 kPa increased by 43%, 17%, and 39% compared with that under 100 kPa, respectively. The bubble spacing factor's increase resulted in a decrease of freeze-thaw resistance of concrete. Thus, under low air pressure, concrete A performed better than J and B in the increase of bubble spacing factor, which kept a better freeze-thaw resistance performance.

4. Conclusions
This paper introduces the synthesis and the performance of novel concrete air-entraining agent----gemini surfactant MRE. The following conclusions are obtained:
-the phenanthrene rings in the MRE led to low arrangement density of molecules at the interface,

MRE has a higher surface activity than the commercially AEA (DCC). The bubble liquid film strength of MRE is 63% higher than that of DCC. The stability of bubbles produced by MRE was better than DCC;

-the air content of concrete with MRE under 60 kPa was only 2% lower than that under 100 kPa, and the bubble spacing factor was 17% higher than that under 100 kPa. After 200 freeze-thaw cycles, the relative dynamic modulus of concrete with MRE decreased less under 60 kPa than DCC. Concrete mixed with MRE had less deterioration in pore structure under low air pressure, and the strength and frost resistance of concrete were less affected under low air pressure. MRE was more suitable for concrete used in the low air pressure environment.

References
1.GELARDI, G., MANTELLATO, S., MARCHON, D., et al. 9 - chemistry of chemical admixtures. Science and Technology of Concrete Admixtures[M], Elsevier, **2016**: 149-218.
2.KHALIL, N., AOUAD, G., CHEIKH, K. E., et al. Use of calcium sulfoaluminate cements for setting control of 3D-printing mortars[J]. *Construction and Building Materials*, 2017, **157**:382-391.
3.NERGIS, D. D. B., VIZUREANU, P., CORBU, O., Synthesis and Characteristics of Local Fly Ash Based Geopolymers Mixed with Natural Aggregates[J]., *Rev. Chim.*, **70**(4), 2019, 1262-1267.
4.ABDULLAH, M. M. A. B., TAHIR, M. F. M., HUSSIN, K., et al. Fly Ash Based Lightweight Geopolymer Concrete Using Foaming Agent Technology[J]. *Rev. Chim.*,**66**(7), 2015, 1001-1003.
5.STANESCU, G. BADANOIU, A., NICOARA, A., et al., Brick and Glass Waste Valorisation in the Manufacture of Aerated Autoclaved Concrete [J]., *Rev. Chim.*,**70**(3), 2019, 828-834.
6. PLANK, J., SAKAI, E., MIAO, C. W., et al. Chemical admixtures-chemistry, applications, and their impact on concrete microstructure and durability[J]. *Cement and Concrete Research*, 2015, **78**:81-99.
7. AÏTCIN, P. C. Science and technology of concrete admixtures [M]. Sawston: Woodhead Publishing, **2016**:87-95.
8. YANG, Q., ZHU, P., WU, X., et al. Properties of concrete with a new type of saponin air-entraining agent [J]. *Cement and Concrete Research*, 2000, **30**(8):1313-1317.
9. MAYERCSIK, N. P., VANDAMME, M., KURTIS, K. E. Assessing the efficiency of entrained air voids for freeze-thaw durability through modeling [J]. *Cement and Concrete Research*, 2016, **88**:43-59.
10. R. GAGNÉ. 17- Air entraining agents [J]. *Science and Technology of Concrete Admixtures*, **2016**:379-391.
11. LI, X., FU, Z. Effect of low-pressure of the environment on air content and bubble stability of concrete [J]. *Journal of the Chinese Ceramic Society*, 2015, **43**(8):1076-1082.
12. LUO, Z., FU, Z., LI, X. Effect of atmospheric pressure on air content and air void parameters of concrete [J]. *Magazine of Concrete Research*, 2015, **67**(8):391-400.
13. LI, Y., WANG, Z., WAMG, L. The influence of atmospheric pressure on air content and pore structure of air-entrained concrete [J]. *Journal of Wuhan University of Technology-Mater Sci Ed*, **2019**(6):1365-1370.
14. QIAO, M., CHEN, J., YU, C., et al. Gemini surfactants as novel air-entraining agents for concrete[J]. *Cement and Concrete Research*, 2017, **100**:40-46.
15. CHEN, J., QIAO, M., GAO, N., et al. Cationic oligomeric surfactants as novel air-entraining agents for concrete [J]. *Colloids and Surfaces A Physicochemical and Engineering Aspects*, **538**:686-693.
16.JIAO, T., LIU X., WANG X., et al. Synthesis and aggregation behaviors of disulfonate gemini surfactant with double hexadecyl tails [J]. *Colloids & Surfaces A Physicochemical & Engineering Aspects*, 2016, **498**:30-41.

17.CHANG, H. H., GAO X. R., WANG, Y., et al. Equilibrium and dynamic surface tension properties of Gemini quaternary ammonium salt surfactants with ester groups[J]. *Colloids & Surfaces A Physicochemical & Engineering Aspects*, 2016, **509**:130-139.

18. KUO, C. F. J., LIN, L. H., DONG, M. Y., et al. Preparation and properties of new ester-linked cleavable gemini surfactants[J]. *Journal of Surfactants and Detergents*, 2011, **14**(2):195-201.

19. ACHARYA, D. P., JOSE, M. G., ARAMAKI, K., et al. Interfacial properties and foam stability effect of novel gemini-type surfactants in aqueous solutions[J]. *Journal of Colloid and Interface Science*, 2005, **291**(1):236-243.

20. ZANA, R. Dimeric and oligomeric surfactants. Behavior at interfaces and in aqueous solution: a review [J]. *Advances in Colloid and Interface Science*, 2002, **97**:205-253.

21. LEI, L. Synthesis and self-organization of rosin-based surfactants [D]. Jiangnan University, 2017.

22. YU, X. New Rosin-based surfactant: effect of rigid hydrophobic structure on its self-organizing behavior [D]. Jiangnan University, 2016.

23. FU, F., WANG, D., SHEN, M. et al. Preparation of radical polymerizablerosinyl benzocyclobutene monomer and its polymerization properties [J]. *Forestry Chemistry and Industry*, **2019**(6): 1-8.

24. ZHAI, Z., GAO, H., SHANG, S., et al. Research progress in the preparation and application of water-soluble rosin resin [J]. *Biomass Chemical Engineering*, 2018, **52** (3): 45-49.

25. LENG, F., DUAN, W., XU, X., et al. Research on a new method for preparing maleic abietic acid [J]. *Chemistry and Industry of Forest Products*, 2011, **31** (5): 65-70.

26. NIU, H., LOU, P., ZHU, H., DING H. Study on synthesis technology of ester-based gemini quaternary ammonium softener [J].] *Fine Chemicals*, 2010, **27**(08):823-827+832.

27.***GBT 14684-2011 Stand for construction[S].

28.***GBT 14685-2011 Pebble and crushed stone for construction[S].

29.***JGJ 63-2006 Water standard for concrete[S].

30. HAN, S. Synthesis and preparation of nanomaterials by rosin-based bisubsurfactant [D]. Northeast Forestry University, 2012.

31. LI, Y., WANG, Z., WANG, L. Effect of low air pressure on bubble generation and development of air-entraining agent solution[J]. *Concrete*, **2019**(08):144-148.

32. MAO, L., HUANG, Z., SHANG, Y., et al. Analysis of air-entraining liquid membrane monolayer and stomatal structure of hardened concrete[J]. *Jiangsu Architecture*, **2010**(6): 89-92.

33.***GBT 50082-2019 Standard for long-term performance and durability test method of ordinary concrete[S].

34. GAO, H., ZHANG, X., ZHANG, Y. Effect of Air Void Structure on Strength and Interfacial Transition Zone of Concrete[J]. *Journal of Tongji University*, 2014, **42**(5): 751-756.